Adsorption of Surfactants at the Gas/Solution Interface of Cavitation Bubbles: An Ultrasound Intensity-Independent Frequency Effect in Sonochemistry

Joe Z. Sostaric* and Peter Riesz*

Radiation Biology Branch, National Cancer Institute, National Institutes of Health, Bethesda, Maryland 20892

Received: September 19, 2002

A major limitation in determining the effects of ultrasound frequency in sonochemistry in relation to cavitation is that no reliable relationship exists between the energy supplied to the system and the energy converted by the cavitation process in producing a sonochemical effect. However, the current study presents a frequency effect that is independent of the energy supplied to the system. Spin-trapping of secondary carbon radicals with 3,5-dibromo-4-nitrosobenzenesulfonic acid-d_2 (DBNBS-d_2) and electron paramagnetic resonance (EPR) have been used to determine the relative ability of two nonvolatile surfactants [sodium 1-pentanesulfonic acid (SPSo) and sodium dodecyl sulfate (SDS)] to scavenge $^{\bullet}$H atoms and $^{\bullet}$OH radicals at the gas/solution interface of cavitation bubbles. The results obtained at 354 and 1057 kHz are compared to those observed previously at 47 kHz (Sostaric, J. Z.; Riesz, P. *J. Am. Chem. Soc.* **2001**, *123*, 11010−11019). At particular bulk surfactant concentrations, both surfactants reached a limiting plateau value in radical scavenging ability. At 354 kHz (and 47 kHz), the magnitude of this plateau was greater for SPSo compared to that for SDS. However, at 1057 kHz, no difference in the plateau value was observed between SPSo and SDS. Decreasing the ultrasound intensity at constant frequency during the sonolysis of SPSo and SDS resulted in a decrease in the $-^{\bullet}$CH− radical yield. However, there was no change in the relative plateau yield of $-^{\bullet}$CH− radicals between SPSo and SDS. Thus, at plateau concentrations, the relative ability of these *n*-alkyl chain surfactants to scavenge radicals at the gas/solution interface of cavitation bubbles depends on the frequency of sonolysis but is independent of ultrasound intensity. The results were interpreted in terms of a decrease in the rate of change of the surface area of "high-energy-stable cavitation bubbles" at higher frequencies. This would affect the relative adsorption and hence radical scavenging efficiencies of SPSo and SDS at the gas/solution interface of these types of cavitation bubbles.

Introduction

The ability of organic solutes to accumulate at the gas/aqueous solution interface of cavitation bubbles is known to play an important role in a number of ultrasound induced/enhanced processes such as the destruction of pollutants and hazardous chemicals,[1−11] polymerization reactions,[12−14] the formation of nanoparticles[15−26] and biomedical applications.[27,28] This includes sonodynamic therapy, the use of ultrasound in combination with certain drugs (sonosensitizers), which has been shown to produce a synergistic effect in the treatment of tumor-bearing animals.[29,30] The experimental evidence suggests that sonosensitization follows the accumulation of the surface-active sonosensitizers at the gas/solution interface of cavitation bubbles.[31−34]

Given the large scope of surfactant use in aqueous sonochemical processes, it is essential to gain a fundamental understanding of the action of surfactants during sonolysis, especially under different sonolysis regimes. For example, it has been proposed that the accumulation of surfactant at the gas/solution interface is influenced by the oscillations of the cavitation bubbles.[35] It has also been shown experimentally using sonochemistry[36] and sonoluminescence[37a] that the equilibrium surface activity of surfactants does not necessarily determine the ability of a surfactant to accumulate at the gas/solution interface of cavitation bubbles but also depends on the dynamics of surfactant accumulation at the interface. Interestingly, recent results by Miyoshi et al.[38] show that cell killing during the in vitro exposure of the human leukemia cell line (HL-60) to 47-kHz ultrasound in the presence of porphyrin molecules to which a homologous series of *n*-alkyl chains were attached may also depend on surfactant dynamics.[38] In addition to these surface chemical effects, it is well known that changes in certain parameters during sonolysis (e.g., solution viscosity, ambient temperature and pressure, saturating gas type, and the frequency and intensity of ultrasound) result in significant changes in the cavitation phenomenon,[39,40] hence the associated chemical and physical effects of the sonochemistry of water.

Over the past decade or so, there has been growing interest in the effect of frequency on acoustic cavitation and its associated sonochemical effects.[7,9,41−59] The main reason for this lies in the potential for enhancing a sonochemical effect for a given energy input to the system, with the wider aim of gaining a better understanding of the underlying cavitation process at different frequencies. However, many aspects of cavitation in the multibubble field change when the frequency of sonolysis is altered. Thus, to study frequency effects during sonolysis, a number of methods have been used with the aim of keeping as many parameters constant during sonolysis as possible. This is especially so with regard to keeping the ultrasound power constant. In the current study, "ultrasound power" is specifically defined as the energy converted by the cavitation process in producing a sonochemical effect.

* Corresponding authors. E-mail: sostarij@mail.nih.gov and sono@helix.nih.gov.

10.1021/jp022106h CCC: $22.00
Published on Web 11/13/2002

A number of techniques have been proposed to standardize the ultrasound power during sonolysis.[39,40,60,61] One method has been to keep the electrical energy to the transducer constant.[9,41] This method will suffice if the aim is solely to determine the frequency at which the greatest yield of a sonochemical process occurs for a certain energy input to the different transducers. However, although the electrical power supplied to the transducer is the same, this definitely does not translate to a proportional conversion of the supplied energy (by the cavitation bubbles) into creating a sonochemical effect at different frequencies. Thus, any attempt to draw conclusions about bubbles in a multibubble cavitation field at different frequencies on the basis of keeping the electrical power to the transducer constant is theoretically flawed.

To overcome this difficulty, sonochemists generally standardize sonochemical results to a calorimetrically determined ultrasound power[40] absorbed by the solution at different frequencies.[7,42−48,53−56] However, this approach for establishing conclusions regarding cavitation bubble dynamics has already been strongly criticized in the literature.[50,51] It is clear that one of the critical parameters that is currently difficult if not impossible to keep constant when sonolysis is conducted at different frequencies is the ultrasound power.[50,51] In an attempt to address this problem, Reisse and co-workers[50,51] adjusted the ultrasound intensities of their apparatus to obtain the same reaction rate for a particular reaction (the reference reaction) at different frequencies and then compared the rate of this reaction to the rate of a second reaction (the test reaction).

This comparative method of determining a frequency effect in sonochemistry was previously used by Petrier et al.[58] However, it has been argued[50,51] that the choices of the reference and test reactions for comparison at different frequencies in that study[58] were too dissimilar. The choice of reactions to examine the frequency effect is critical since it is known that three different regions of chemical activity exist during the sonolysis of water: the interior of the collapsed bubble where pyrolysis occurs at about 5000 K,[62] the hot shell surrounding the hot spot, where solutes can undergo pyrolysis and radical scavenging reactions at approximately 1900 K,[62] and the bulk solution at ambient temperature.[62] Thus, to observe a true frequency effect in sonochemistry (which can be related to a frequency effect on cavitation) would at least necessitate that both the test and reference reactions are occurring in the same region. For example, comparing the rate of a radical process at the interface with the rate of thermal decomposition of a volatile solute occurring in the collapsing bubble would be of limited value for determining a frequency effect in sonochemistry. This is because, at the very least, these processes would depend on the surface activity and volatility of the solutes, respectively. Thus, it would be difficult to determine what aspect of cavitation changed to create the frequency effect.

For this reason, Dekerckheer et al.[50] considered two reactions with a similar primary initiation step during sonolysis (i.e., either the homolytic cleavage of CCl_4 (in the Weissler reaction) or Br_2 (in the isomerization of maleic to fumaric acid) at ultrasound frequencies of 20 kHz and 1.7 MHz). However, even this choice of reference and test reactions would have limitations for determining how cavitation bubbles are affected by frequency changes[63] since there are still numerous physical and chemical parameters that have not been kept constant. These include the volatility, surface activity, bond energies of the reactants, and reaction rate of the processes being studied, all of which may affect the reactions to different degrees and for various reasons at different frequencies.

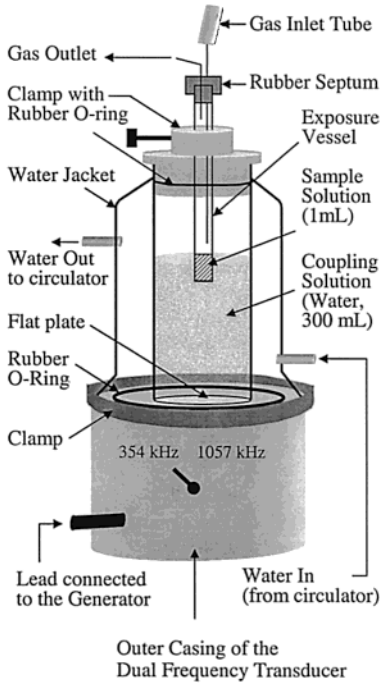

Figure 1. Experimental apparatus for sonolysis at 354 and 1057 kHz.

In the current study, the primary $^{\bullet}H$ and $^{\bullet}OH$ radical scavenging efficiency of two *n*-alkyl chain, anionic surfactants—SPSo and SDS—is compared at ultrasound frequencies of 354 kHz and 1057 kHz in aqueous argon-saturated solutions using the same sonochemical apparatus (Figure 1). Both sonochemical processes are identical with respect to the region of the sonochemical reaction (i.e., the gas/solution interface of cavitation bubbles) and are also chemically similar (i.e., the abstraction of H atoms from the *n*-alkyl chain). To observe a frequency effect, this study focuses on a physical chemical parameter that is not kept constant during sonolysis, which is the ability of SPSo and SDS to accumulate at the dynamic gas/solution interface of cavitation bubbles. For the analysis of the elusive frequency effect in sonochemistry, we have made no attempt to standardize the ultrasound power at the two frequencies because, as shall be shown, the effects observed are independent of the ultrasound power.

Experimental Section

Materials. 3,5-Dibromo-4-nitrosobenzenesulfonic acid-d_2 (DBNBS-d_2) was obtained from Dr. Miles Chedekel's Melanin Laboratories. Sodium 1-pentanesulfonic acid (SPSo) was purchased from the Sigma Chemical Co. Sodium dodecyl sulfate (SDS, ≥99%) was obtained from Fluka Chemika. All solutions were made with Milli-Q filtered water (conductivity $<10^{-6}$ S cm^{-1} and surface tension of 72.0 mN m^{-1} at 25 °C). Glassware was washed using Extran 300 detergent supplied by Electron Microscopy Sciences.

Sonolysis Experiments. All glassware was washed prior to use with Extran 300 detergent, left to soak in concentrated nitric acid (1 h), and then rinsed thoroughly with Milli-Q water. The ultrasound transducer (model USW 51) and RF power generator (model LVG 60) were purchased from L-3 Communications ELAC Nautik GmbH. The experimental setup is shown in Figure 1. The transducer unit operated at one of two frequencies (354 or 1057 kHz) and transmitted the ultrasonic wave to a stainless steel flat plate that was in direct contact with the sonolysis bath coupling solution (300 mL of Milli-Q water).

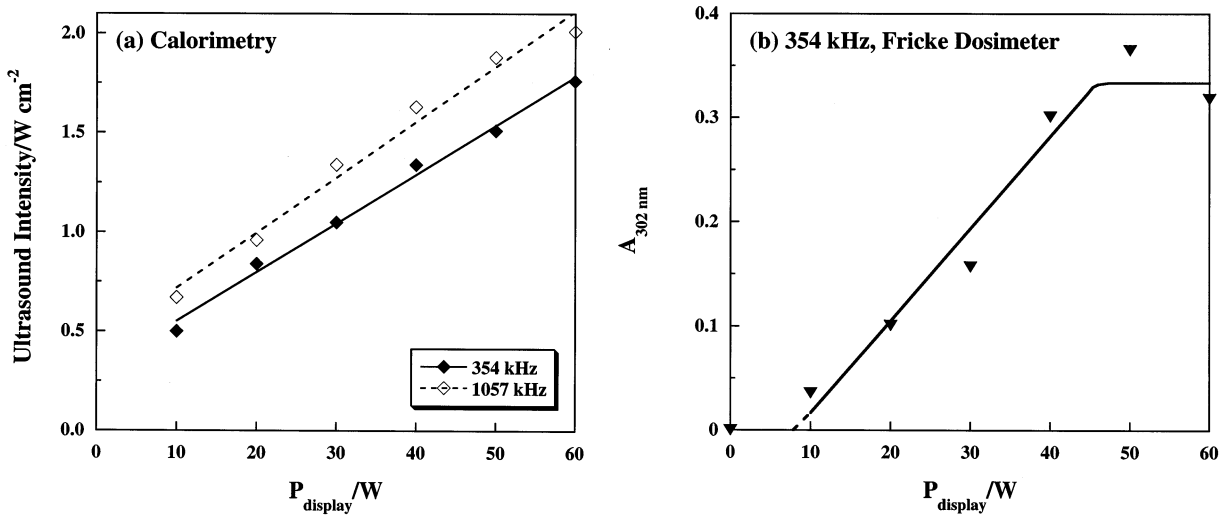

Figure 2. (a) Relationship between the calorimetrically determined ultrasound power input to the 300-mL coupling solution (see Figure 1) and the generator power, $P_{display}$, following sonolysis for 1 min at 354 and 1057 kHz. Solutions were exposed to air; the initial solution temperature was 20.0 ± 0.2 °C. (b) Absorbance (302 nm) of the Fricke dosimeter solution following sonolysis at 354 kHz at various generator powers $P_{display}$. Conditions: argon-saturated, T = 20.0 ± 0.2 °C, time of sonolysis = 3 min.

The sonolysis bath cell was surrounded by a Pyrex water jacket that was connected to a self-regulating water circulator (model DC50) and cooling bath (model K20) supplied by Haake (USA). A temperature of 20 °C was maintained by sonicating the coupling solution for 10 min prior to every sonolysis experiment and setting a previously determined operating temperature on the Haake cooling system, which depended on the frequency and intensity of sonolysis. During the 10 min of sonolysis, the coupling solution reached a steady-state temperature of better than 20.0 ± 0.2 °C.

Fresh sample solutions for sonolysis were prepared and placed in a custom-made cylindrical Pyrex exposure vessel with external dimensions of 13 mm × 140 mm. The exposure vessel had a flat bottom and a wall thickness of 1 mm. It was positioned reproducibly above the flat plate and in the center of the main sonolysis bath with a specially designed clamp that was firmly attached to the top of the sonolysis bath cell. Prior to sonolysis, the exposure vessel was sealed using a rubber septum ("suba seal", supplied by Aldrich) and bubbled with argon gas for 5 min. During this time, the sample solution was allowed to reach an equilibrium temperature of 20.0 ± 0.2 °C by suspending the exposure vessel in a water bath. Following argon bubbling, the gas supply tube was raised to allow argon to pass over the top of the solution, the exposure vessel was clamped into position in the presonicated bath, and sonolysis was conducted for either 3 min (354 kHz) or 5 min (1057 kHz) unless otherwise indicated.

Characterization of the Sonochemical System. The ultrasound power intensity was determined calorimetrically[64] (Figure 2a) by measuring the temperature rise in the 300-mL coupling solution (see Figure 1) following 1 min of sonolysis with a flat plate of area 25 cm^2. The measurements were conducted with air as the insulating material in the jacket surrounding the main vessel (see Figure 1) and at various values of $P_{display}$ (the electrical power supplied to the transducer as shown on the display of the RF power generator). The measured change in temperature following sonolysis was reproducible within ±0.05 °C at each $P_{display}$ setting (Figure 2a), which relates to an error of less than 5%. The Fe^{3+} yield was also determined following the 354-kHz sonolysis of the Fricke dosimeter[65] for 3 min under argon gas by following the increase in absorbance at 302 nm (Figure 2b). This is a measure of the Fe^{3+} yield due to the effect of ultrasound experienced by the sample in the exposure vessel for the particular range of $P_{display}$ to be considered in this study. At 1057 kHz, the sensitivity of the Fricke dosimeter was too low to detect any sonochemistry. However, the calorimetrically determined ultrasound intensity in the 300-mL coupling solution is greater for 1057 kHz than for 354 kHz sonolysis (Figure 2a). Thus, calorimetry cannot be used to determine the amount of sonochemical activity in the exposure vessel (Figure 1).

It should be noted that the graphs in Figure 2 are not presented here to standardize the system in terms of the ultrasound power (as defined in this paper) as the frequency is varied but to present as much information about the system as possible. Data relating to ultrasound power is presented in this study as a function of the electrical energy being supplied to the transducer ($P_{display}$). This can be compared to the calorimetrically determined ultrasound power intensity in the 300-mL coupling solution (at 354 and 1057 kHz) or to the Fe^{3+} yield in the exposure vessel (at 354 kHz) by referring to Figure 2.

EPR Measurements. The sample solutions containing the surfactant and DBNBS-d_2 (2.7 mM) were removed immediately following sonolysis and transferred to a standard EPR quartz flat (60 mm × 10 mm × 0.25 mm) cell. EPR spectra were recorded at room temperature on a Varian E-9 X-band spectrometer with a 100-kHz modulation frequency. The acquisition, analysis, and simulation of the EPR spectra were conducted using a software program (EPRDAP) written by Dr. P. Kuppusamy (U.S. EPR Inc., Clarksville, MD). The typical instrument settings for the acquisition of the data were as follows: microwave power, 20 mW; modulation amplitude, 1 G; time constant, 0.128 s; scan speed, 50 G/min. The decay of the radical adducts observed was not significant during the measurement time.

Results

Reaction of Primary Radicals with Surfactants during Sonolysis. The sonolysis of the nonvolatile *n*-alkyl chain surfactants, SPSo and SDS, at 354 and 1057 kHz produced EPR spectra with splitting patterns that were almost entirely due to the $-^{\bullet}CH-$ radical adduct of DBNBS-d_2. A list of the type of carbon-centered radicals spin-trapped following the sonolysis of the surfactants and their nitrogen (a_N) and hydrogen (a_H) hyperfine coupling constants is given in Table 1.

TABLE 1: Hyperfine Coupling Constants (Hfccs) of Radicals Spin-Trapped Using DBNBS-d_2 during the Sonolysis of Aqueous Surfactant Solutions

surfactant	radical type	position[b]	Hfccs/G[a] a_N	Hfccs/G[a] a_H
SPSo	$^{\bullet}CH_2R$		14.4	12.2(2)
	R$^{\bullet}$CHR′	*x*CH	14.4	8.2
	R$^{\bullet}$CHR′	*y*CH	13.8	7.6
SDS	$^{\bullet}CH_2R$		14.4	12.2(2)
	R$^{\bullet}$CHR′	*x*CH	14.6	8.2
	R$^{\bullet}$CHR′	*y*CH	13.8	7.8

[a] Numbers in parentheses indicate the number of equivalent protons in the spin adduct. [b] Radicals located on the carbon atoms in the center (xCH) and near the terminal end (yCH) of the *n*-alkyl chain of the surfactant.

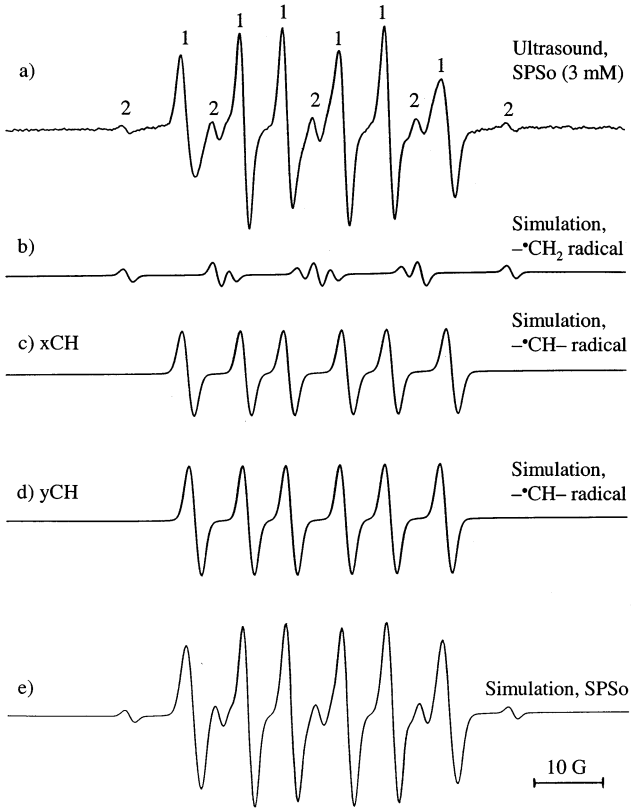

Figure 3. EPR spectrum following the 354-kHz sonolysis of (a) SPSo (3 mM) in the presence of DBNBS-d_2 (2.7 mM). The component signal of the acquired spectrum has been simulated and represents (b) a $-^{\bullet}CH_2$ (labeled 2) radical and two overlapping $-^{\bullet}CH-$ radicals (labeled 1), (c) xCH located away from the terminal carbon atoms of the *n*-alkyl chain, and (d) yCH located near the terminal carbon atoms of the *n*-alkyl chain. The complete simulation of the acquired spectrum is shown in (e). Conditions: argon-saturated, $T = 20.0 \pm 0.2$ °C, time of sonolysis = 3 min, $P_{display} = 60$ W.

The EPR spectrum observed following the 354-kHz sonolysis of an SPSo solution (3 mM) for 3 min under argon and in the presence of DBNBS-d_2 (2.7 mM) is shown in Figure 3a. This spectrum was simulated (Figure 3e) as a contribution of a $-^{\bullet}CH_2$ radical (Figure 3b) and two different types of $-^{\bullet}CH-$ radicals (denoted xCH and yCH in Figure 3c and d, respectively) using the coupling constants shown in Table 1 for SPSo, 354 kHz. It was not possible to simulate the spectra using just one type of $-^{\bullet}CH-$ radical adduct. The formation of two types of $-^{\bullet}CH-$ radicals is due to the position of $^{\bullet}OH$ and $^{\bullet}H$ attacks on the *n*-alkyl chain of the surfactant molecule. The $-^{\bullet}CH-$ radical possessing the larger coupling constants (xCH) may be located on any one of the carbon atoms away from the terminal position of the *n*-alkyl chain. The rationale for this is that the (CH_2) groups and the resulting $-^{\bullet}CH-$ radicals that are farther removed from the terminal positions of the *n*-alkyl chain are likely to be more sterically hindered than those that are near the terminal end. The carbon atoms in an alkyl chain will have close to an sp^3 hybridization, but any distortion to lower symmetry will change the relative ratio of the s and p character of the valence-state orbitals on the carbon atom. In ideal tetrahedral symmetry, the hybridization is sp^3, and the orbital of the unpaired electron has 25% s character. Any distortion due to nonequivalent ligands or steric effects can change the hybridization ratio only to somewhere between sp^3 to sp^x (where $x < 3$), leading to an increase in the s character. In the case of sp^2 (where an extreme distortion has "flattened out" the geometry around the valence state of the carbon atom), the s character increases to 33.3%. Such an argument has been well documented in deriving dihedral angles of AX_2- and AX_3-type radicals, where the hybridization ratios derived from the isotropic and anisotropic part of the EPR hyperfine couplings have been successfully employed in predicting deviations in local symmetry.[66] It is proposed that the $-^{\bullet}CH-$ groups in the center of the *n*-alkyl chain are subjected to more distortion than their counterparts ($-^{\bullet}CH-$ groups near the terminal end), leading to a marginal increase in the s character of the former. This results in two magnetically distinct $-^{\bullet}CH-$ radicals, as evidenced from our simulation. The resulting increase in s character would account for an increase in the a_N and a_H hyperfine coupling constants for primary carbon radicals that are located at the center of the *n*-alkyl chain (xCH) compared to the ones that are formed near the terminal end (yCH). The xCH and yCH radicals detected for SPSo following sonolysis were mixed in a 0.78:1 ratio (xCH/yCH) to yield the simulation shown in Figure 3e. It is clear from Figure 3 that radical abstraction reactions are prominent and that methyl radical production following pyrolysis of the surfactant is negligible.

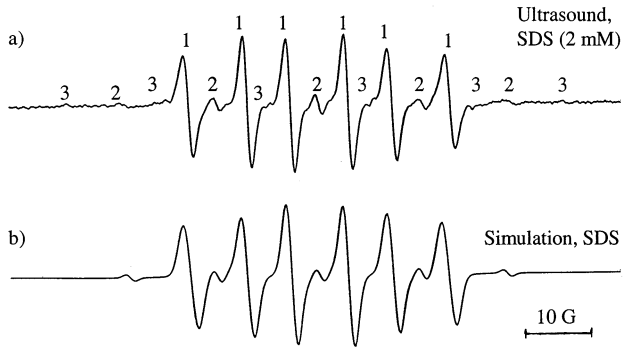

Figure 4. EPR spectrum following the 354-kHz sonolysis of (a) SDS (2 mM) in the presence of DBNBS-d_2 (2.7 mM). Conditions: argon-saturated, $T = 20.0 \pm 0.2$ °C, time of sonolysis = 3 min, $P_{display} = 60$ W. The lines in the spectrum represent methyl (labeled 3), $-^{\bullet}CH_2$ (labeled 2), or two overlapped $-^{\bullet}CH-$ radicals (labeled 1), *x*CH (located in the middle of the *n*-alkyl chain), and yCH (located on the terminal carbon atoms). (b) Computer simulation of the spectrum in Figure 4a (the methyl radical was not simulated).

The EPR spectra acquired following the sonolysis of 2 mM SDS (Figure 4a) in the presence of DBNBS-d_2 were simulated in Figure 4b as a contribution of a ($-^{\bullet}CH_2$)-type radical and two ($-^{\bullet}CH-$)-type radicals with the coupling constants shown in Table 1. The small contribution from methyl radicals was not simulated. In the case of SDS, the ratio xCH/yCH for SDS was 1:1. This result is consistent with the hypothesis of two types of $-^{\bullet}CH-$ radicals being formed since for SDS there are

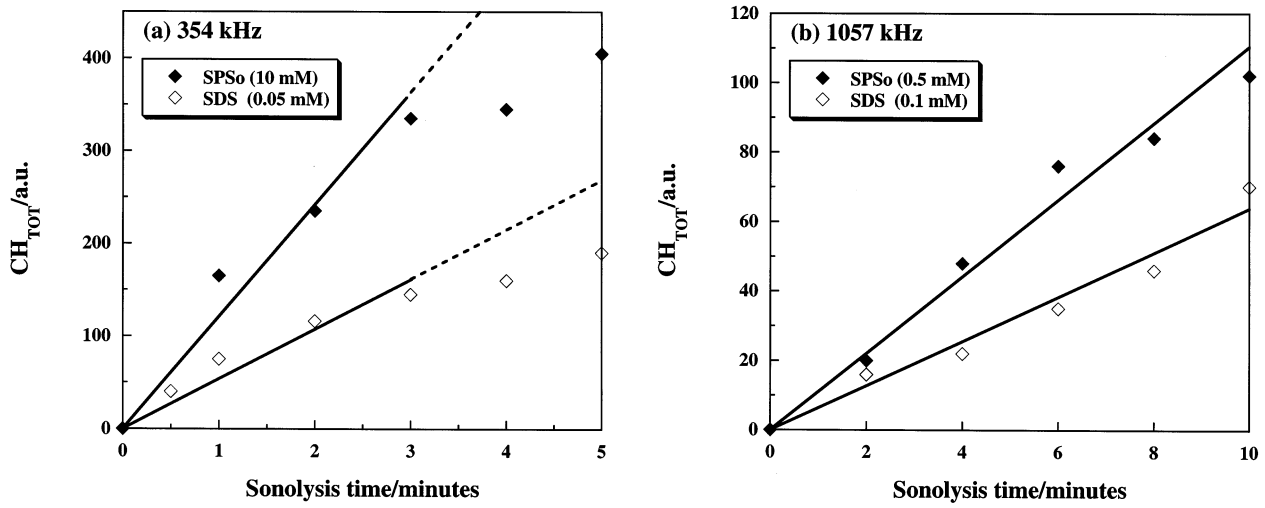

Figure 5. Effect of sonolysis time on the total $-^{\bullet}CH-$ radical yield (CH_{TOT}) observed following the sonolysis of (a) SPSo (10 mM) and SDS (0.05 mM) at 354 kHz and (b) SPSo (0.5 mM) and SDS (0.1 mM) at 1057 kHz. Conditions: [DBNBS-d_2] = 2.7 mM, argon-saturated, $T = 20.0 \pm 0.2$ °C, $P_{display} = 60$ W.

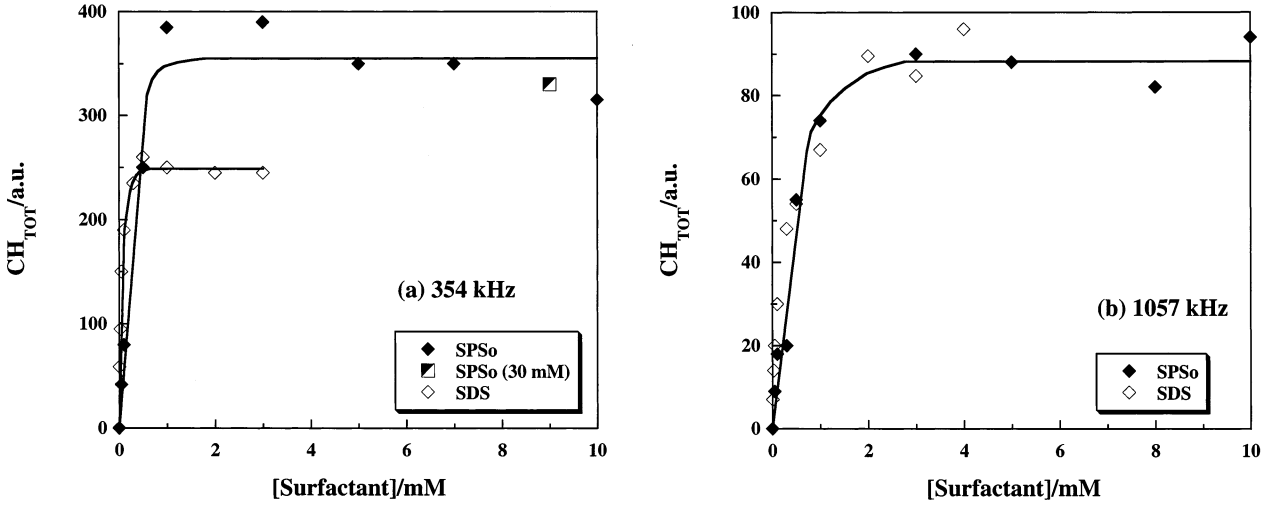

Figure 6. Total $-^{\bullet}CH-$ radical yield (CH_{TOT}) as a function of the concentration of surfactant in bulk solution. Sonolysis frequency: (a) 354 kHz, 3 min and (b) 1057 kHz, 5 min. Conditions: [DBNBS-d_2] = 2.7 mM, argon-saturated, $T = 20.0 \pm 0.2$ °C, $P_{display} = 60$ W.

considerably more C atoms in the center of the *n*-alkyl chain compared to SPSo, so it can be expected that the xCH/yCH ratio should increase because of the increased statistical probability of abstraction occurring in the center of the chain.

When sonolysis was conducted at 1057 kHz, the EPR spectra (not shown) of all of the surfactants looked similar to those obtained following 354-kHz sonolysis. However, the overall radical yield was lower, and so the $-^{\bullet}CH_2$ radicals, which have a low contribution even at 354 kHz, were not as evident following sonolysis at the higher frequency.

Effect of Frequency on Radical Yields Following Sonolysis of *n*-Alkyl Chain Surfactants. To determine the total yield of $-^{\bullet}CH-$ radicals (CH_{TOT}), one would normally doubly integrate the derivative EPR spectrum and measure the area under the absorption. In view of overlap in the spectra due to the presence of two types of $-^{\bullet}CH-$ radicals, we measured the area under the low-field half of the low-field peak of the overlapped $-^{\bullet}CH-$ radical. It should be noted that essentially the same relative radical yields were obtained whether we used the heights of the spectral lines or the area of the low-field half of the doubly integrated spectrum. It was not of interest to determine the absolute yield of radicals produced, as the main aim of this study is to make relative comparisons of CH_{TOT} following sonolysis of the different surfactants under various conditions. CH_{TOT} values for SDS (0.05 mM) and SPSo (10 mM) as a function of the time of sonolysis at $P_{display} = 60$ W and a frequency of 354 kHz are shown in Figure 5a. Similar experiments were conducted at 1057 kHz for SDS (0.1 mM) and SPSo (0.5 mM) (Figure 5b). CH_{TOT} is directly proportional to the sonolysis time for the case of 354 kHz up to at least 3 min of sonolysis (Figure 5a) and for the case of 1057 kHz for up to 10 min of sonolysis (Figure 5b). From the results of Figure 5, the use of spin-trapping and EPR as a quantitative measure of the radical yield is justified for a total time of 3 min during 354-kHz sonolysis and 5 min during sonolysis at 1057 kHz.

The effect of SDS and SPSo on CH_{TOT} in the bulk solution concentration range of 0 to 10 mM is shown in Figure 6a and b for $P_{display} = 60$ W and frequencies of 354 and 1057 kHz, respectively. At 354 kHz (Figure 6a) as the surfactant concentration is increased, CH_{TOT} increases to a maximum plateau yield that is greater for SPSo than for SDS. This result is consistent with those reported previously for the sonolysis of similar surfactant solutions at a frequency of 47 kHz[36] and is not consistent with the order that would be expected from a consideration of equilibrium absorption of surfactants at the gas/solution interface.[36] At 1057 kHz, however (Figure 6b), a

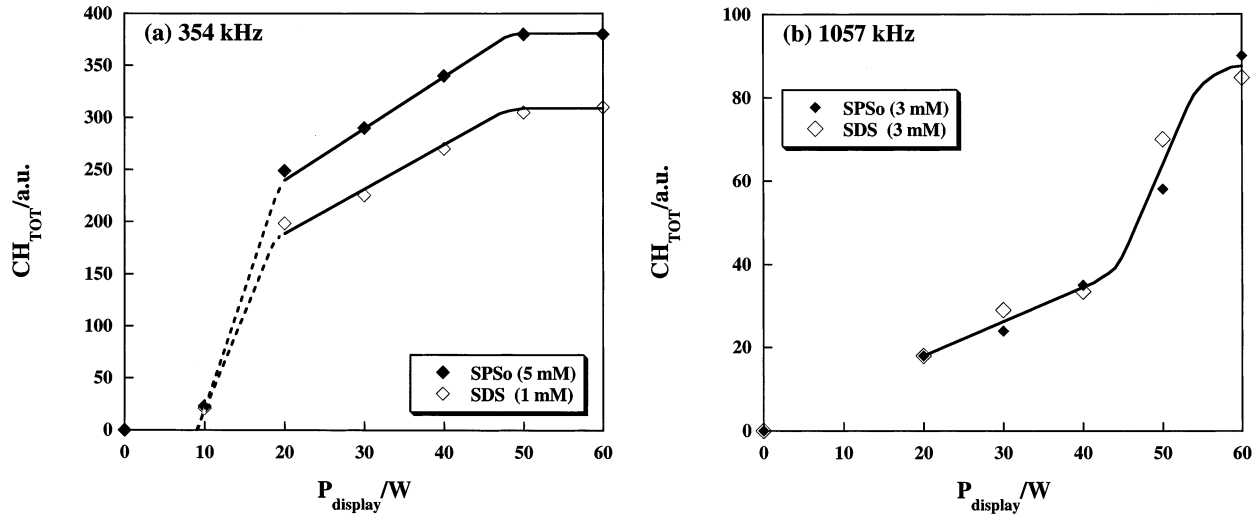

Figure 7. Total $-^{\bullet}CH-$ radical yield (CH_{TOT}) as a function of the generator power input to the transducer ($P_{display}$) during the sonolysis of (a) SPSo (5 mM) and SDS (1 mM) at 354 kHz for 3 min and (b) SPSo (3 mM) and SDS (3 mM) at 1057 kHz for 5 min. Conditions: [DBNBS-d_2] = 2.7 mM, argon-saturated, $T = 20.0 \pm 0.2$ °C.

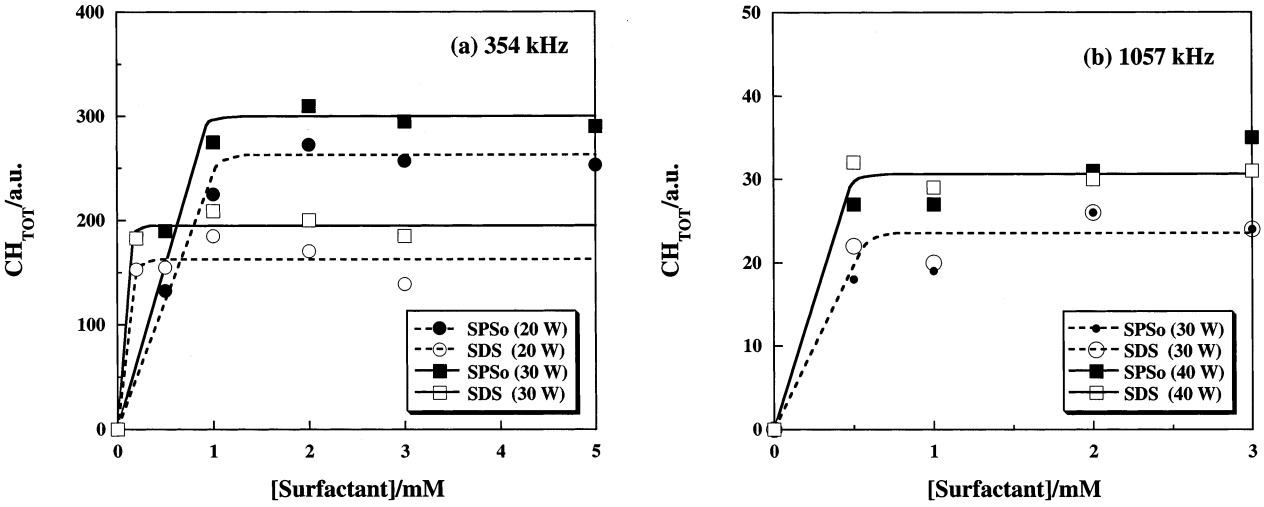

Figure 8. Total $-^{\bullet}CH-$ radical yield (CH_{TOT}) as a function of the concentration of surfactant in bulk solution and the generator power input to the transducer ($P_{display}$). Sonolysis frequency: (a) 354 kHz, 3 min and (b) 1057 kHz, 5 min. Conditions: [DBNBS-d_2] = 2.7 mM, argon-saturated, $T = 20.0 \pm 0.2$ °C.

limiting plateau value in CH_{TOT} is observed that is equal, within experimental error, for both of the surfactants.

Effect of Ultrasound Intensity on Radical Yields at Constant Frequency. To establish that a true frequency effect has been observed following the sonolysis of the surfactant solutions (Figure 6), it is essential to understand the effect of ultrasound intensity ($P_{display}$) on the radical yields at constant frequency. The effect of $P_{display}$ on a single concentration of SDS and SPSo (chosen from the plateau values in Figure 6) was considered at frequencies of 354 and 1057 kHz, as shown in Figure 7a and b, respectively. To further investigate the ultrasound intensity effect, CH_{TOT} was measured as a function of the surfactant concentration at lower generator powers for both frequencies, as shown in Figure 8a (354 kHz) and b (1057 kHz). This data is similar to that presented in Figure 6 at the higher power, $P_{display} = 60$ W. As the generator power was decreased, the total yield of radicals decreased at all concentrations; however, the profile of the curves (Figures 6 and 8) remained similar for both surfactants.

Discussion

Mechanism of $-^{\bullet}CH-$ Radical Formation during the Sonolysis of Surfactants. The trends observed for the number of $-^{\bullet}CH-$ radicals trapped by DBNBS-d_2 during sonolysis can be explained by considering the primary radical processes that result in the formation of the radical adduct. This question has been addressed in detail in a previous study,[36] where it was shown that the yield of the $-^{\bullet}CH-$ radical adduct determined following the sonolysis of surfactant solutions at a frequency of 47 kHz correlates with the amount of surfactant that can accumulate at the gas/solution interface of cavitation bubbles. In essence, the violent collapse of cavitation bubbles in aqueous solutions results in the formation of $^{\bullet}OH$ radicals and $^{\bullet}H$ atoms.[67,68] In argon-gassed solutions, these radicals recombine to produce H_2O_2, H_2, and H_2O. However, when a nonvolatile organic solute is added to the solution, a portion of the $^{\bullet}OH$ radicals and $^{\bullet}H$ atoms can be scavenged to produce carbon centered radicals that react with the spin trap in the bulk solution.[69] At the low bulk solution concentrations of nonvolatile surfactant used in this study, essentially all of the primary radicals are being scavenged at the gas/solution interface of the cavitation bubbles with little, if any, scavenging occurring in the bulk solution.[36,69] Therefore, CH_{TOT} is a measure of the concentration of surfactant at the gas/solution interface of cavitation bubbles.

Effect of Ultrasound Frequency on the Relative CH_{TOT} Yields Following Sonolysis. The 354-kHz results (Figures 6a and 8a) show that the anionic surfactant possessing the shortest *n*-alkyl chain length (SPSo) was more efficient at accumulating at the gas/solution interface of cavitation bubbles (at the plateau concentrations) in comparison to the more surface-active molecule (SDS). These results are similar to previous observations made following the sonolysis of surfactant solutions at 47 kHz (radical yield determination)[36] and 358 kHz (sonoluminescence).[37a] This observation could be explained by considering the surfactant adsorption dynamics at the gas/solution interface of cavitation bubbles. Surfactant molecules require a finite time to attain equilibrium between the gas/solution interface and the bulk solution.[70] This may be due to a combination of factors including diffusion to the interface from the bulk solution and overcoming a number of barriers to adsorption such as increased surface pressure, fewer vacant sites being available for adsorption, and being in the correct orientation for adsorption to take place.[70] Thus, it was concluded that relatively high molecular weight surfactants could not establish equilibrium at the rapidly expanding and contracting interface of cavitation bubbles.[36] Furthermore, compared to SPSo, SDS possesses a higher equilibrium surface excess (Γ_{eq}) at a particular bulk concentration and hence requires longer times to establish equilibrium between the gas/solution interface and the bulk.[71] It was proposed that SPSo could reach substantially higher concentrations at the interface of cavitation bubbles because of its more-efficient adsorption dynamics compared to that of SDS.[36]

In contrast to the observations made at 47-kHz[36] and 354-kHz (Figure 6a) sonolysis, similar maximum radical scavenging yields were realized for both surfactants during sonolysis at 1057 kHz (Figure 6b). An explanation (see the final discussion section for details) for the observation at 1057 kHz (Figure 6b) is that the adsorption of surfactants at the gas/solution interface of cavitation bubbles is facilitated in comparison to adsorption at the lower frequencies.

For clarity, a comparison of the radical yields measured for SPSo and SDS following sonolysis at all three frequencies is shown in Figure 9. This Figure was generated by normalizing the data for CH_{TOT} observed for SDS and SPSo at the three frequencies (ref 36 and Figure 6a and b) to an average SDS plateau value that was calculated from the data points that lie on the plateau for SDS at each frequency. Thus, the normalized SDS plateau value becomes equal to approximately 1 (within the error of the experiment) at all frequencies, to which the relative $-^{\bullet}CH-$ radical yield at the plateau following the sonolysis of SPSo solutions can be compared. It can be deduced from Figure 9 that the enhanced ability of SPSo to accumulate at the gas/solution interface of cavitation bubbles, compared to that of SDS at low frequencies, decreases as the frequency is increased. In comparison to SDS, SPSo was almost twice as efficient a radical scavenger at 47 kHz, approximately 1.5 times as efficient at 354 kHz, but had the same limiting radical-scavenging efficiency at 1057 kHz. However, it should be noted that the 47-kHz results were conducted in an ultrasonic bath.[36]

The separation between the plateau values of CH_{TOT} for SPSo and SDS has increased from 354 to 47 kHz (Figure 9), but to show that this effect is independent of the configuration of the sonolysis apparatus[48,50] would require further investigation. For this reason, no attempt is made to address the difference in plateau heights between SPSo and SDS at 354 and 47 kHz (Figure 9) except to say that the results of the 47-kHz study,[36] showing that SPSo is a more effective radical scavenger compared to SDS, do correspond well to the results observed

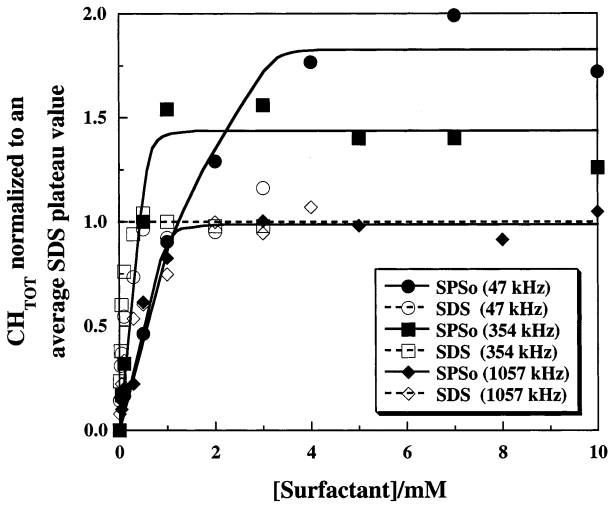

Figure 9. Effect of the surfactant concentration on the relative $-^{\bullet}CH-$ radical yields at various frequencies. Data have been normalized to an average SDS plateau value of 1 at all frequencies (see text). Conditions for 354 and 1057 kHz were [DBNBS-d_2] = 2.7 mM, argon-saturated solutions, $T = 20.0 \pm 0.2$ °C, and $P_{display} = 60$ W. Sonolysis results at 47 kHz were analyzed from an earlier study,[36] which was conducted in the presence of DBNBS (8.2 mM) in an ultrasonic bath. The bath sonolysis conditions were argon-saturated solutions, $T = 20 \pm 1$ °C, and time of sonolysis = 5 min.

at 354 kHz in the current study (Figure 9). The observation that both surfactants have the same limiting radical-scavenging efficiency at 1057 kHz (Figure 9) is clearly a different result from that described above. However, to show that this effect is due to a change in the ultrasound frequency, the effect of ultrasound power on these absorption efficiencies must be established.

Effect of Ultrasound Intensity on the Relative CH_{TOT} Yields at Constant Frequency. There are a number of similarities between the curves in Figure 7 (and the dosimetry results of Figure 2b) and previously reported data for various sonochemical reactions.[48,72] In general, the radical yield approaches zero at well above zero generator power because of a cavitation threshold.[39,73a,b] At generator powers that are too low, too few or no effective cavitation events occur for sonochemistry to be detected. At the higher powers, 50 to 60 W (Figures 2b and 7), a plateau in the sonochemical yield is approached. This effect has also been reported previously[48,72] and can be explained in terms of bubbles now beginning to grow too large to undergo violent collapse[72] or by the onset of an acoustic impedance mismatch, which is brought about by intense cavitation around the transducer.[73c] An interesting observation is made when the relative radical yields for SPSo and SDS are compared as a function of ultrasound power ($P_{display}$) at 354 kHz (Figure 10a) and 1057 kHz (Figure 10b).

Figure 10 was produced in a similar way to Figure 9. The data from Figures 6 and 8 were normalized to an average SDS plateau value calculated from the data points that lie on the plateau for SDS, allowing for a comparison of the relative numbers of radicals produced with varying $P_{display}$ (Figure 10). Although $P_{display}$ had a large effect on CH_{TOT} (Figure 7), the relative yield of radicals formed for SPSo compared to SDS at the plateau concentrations of the surfactant does not change over the whole ultrasound power range, irrespective of the sonolysis frequency (Figure 10). Only a change in the ultrasound frequency has created an effect (Figure 9). The broader implications of these results are discussed in the following section.

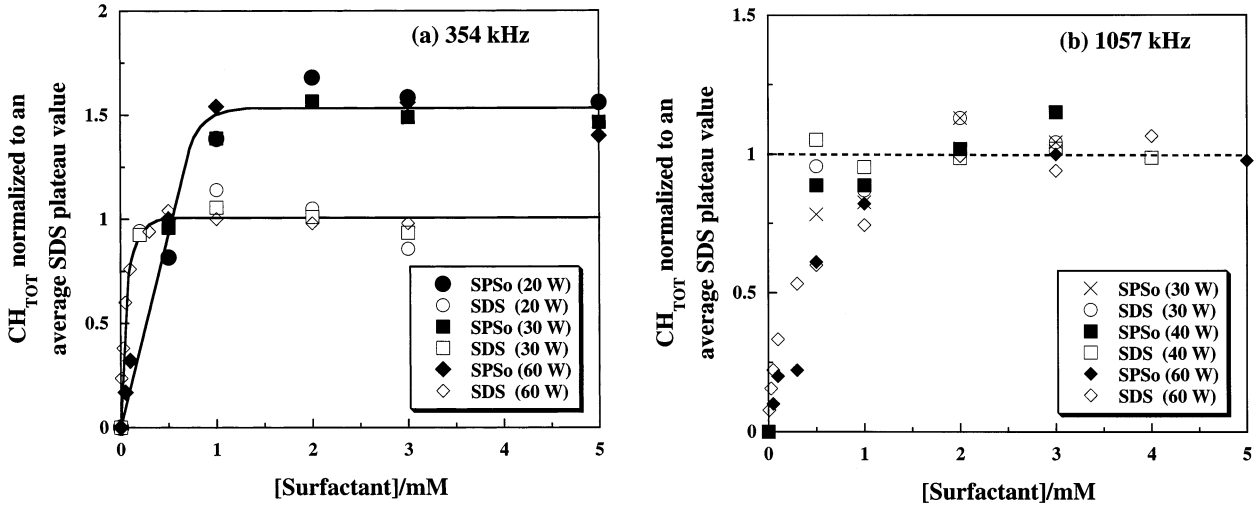

Figure 10. Effect of surfactant concentration on the relative $-^{\bullet}CH-$ radical yields at various generator power inputs to the transducer. Data have been normalized to an average SDS plateau value of 1 at all ultrasound intensities (see text). Sonolysis was conducted at (a) 354 kHz for 3 min and (b) 1057 kHz for 5 min. Conditions: [DBNBS-d_2] = 2.7 mM, argon-saturated, $T = 20.0 \pm 0.2$ °C.

TABLE 2: Description of Cavitation Bubbles that Can Produce Sonochemistry at Various Frequencies

frequency/kHz	47		354		1057	
R_r/μm[a]	76		10		3.4	
bubbles that create	HES	transient	HES	transient	HES	transient
sonochemistry	yes	yes	yes	yes	yes	no
lifetime[b] prior to collapse (τ)/ms	2−20	0.02−0.06	0.3−3	0.003−0.009	0.1−0.9	($\sim 3 \times 10^{-3}$)

bubble oscillation amplitude: variation from R_r (%)	$[\Delta A_s(R_{comp} \leftrightarrow R_{exp})_t/10^{-3}$ m^2 s$^{-1}]$[c]	
10	0.36	0.12
20	0.72	0.24
30	1.08	0.36
40	1.44	0.48
50	1.80	0.60

[a] Approximate values of the resonance radii of the bubbles, calculated using eq 1. [b] Calculated assuming that HE-stable bubbles exist for 100 to 1000 acoustic cycles prior to undergoing collapse and that the transient bubbles exist for just 1 to 3 acoustic cycles. [c] Approximate time-averaged rate of change of the gas/solution interfacial area of HE-stable bubbles during oscillations between the maximum compression (R_{comp}) and expansion (R_{exp}) radii—see eq 2.

Effect of Frequency and Intensity of Ultrasound on Cavitation Bubbles. (i) Description of Cavitation Bubbles in a Multibubble Field. The current discussion is limited to the two types of cavitation bubbles that can eventually create sonochemistry. The description presented by Leighton[73d] shall be followed, where high-energy-stable cavitation (HE-stable bubbles) refers to cavitation bubbles that can oscillate for many acoustic cycles to eventually undergo violent collapse, create sonochemistry, and then reform. Thus, stable cavitation bubbles that do not create sonochemistry will not be considered here. Second, transient cavitation refers to cavitation bubbles that exist for less than a few acoustic cycles, grow rapidly, and then undergo inertial collapse resulting in sonochemistry and the fragmentation of the original bubble.

Table 2 describes in more detail the probable types of cavitation bubbles that create sonochemistry at 47, 354, and 1057 kHz. An approximation for the resonance radius (R_r) of the cavitation bubbles has been calculated[73e] at each frequency using eq 1:

$$R_r = \frac{1}{2\pi f_r}\left(\frac{3\gamma P_h}{\rho} - \frac{2\sigma}{\rho R_r}\right)^{1/2} \qquad (1)$$

where the ratio of the specific heats of argon gas $C_p/C_v = \gamma = 1.66$, the hydrostatic pressure (P_h) = 1.013×10^5 N m^{-2}, the density of the liquid (ρ) = 1000 kg m^{-3}, f_r is the ultrasound frequency, and σ the surface tension of the liquid. The Laplace pressure term in eq 1 ($2\sigma/R_r$) can be neglected because it has a relatively small effect on the calculation for the range of frequencies (47 to 1057 kHz) and surface tension values (approximately 72 to 55 mN/m) considered in the current study.

On the basis of the assumptions that HE-stable bubbles can exist for hundreds of acoustic cycles prior to undergoing collapse (i.e., 100−1000 acoustic cycles) and that transient bubbles have a lifetime only 1−3 acoustic cycles,[74] the lifetime of transient and HE-stable bubbles have been calculated at different frequencies and are also presented in Table 2. It should be noted that this assumption results in a HE-stable bubble lifetime that is longer at lower than at higher frequencies (Table 2). In a real system, however, the opposite may be true. This could be due to a number of reasons (not discussed here) that make it more difficult for bubbles to undergo transient collapse at higher frequencies,[40a,54,56,75] thus increasing the lifetime of HE-stable bubbles prior to collapse. Nevertheless, the lifetimes shown in Table 2 allow for a comparison between HE-stable and transient bubble lifetimes at a particular frequency. At 1057 kHz, the negative pressure cycle of the wave exists for just 0.5 μs, which is comparable to bubble collapse times.[76] Hence, little time is available during the rarefaction cycle of the wave for bubbles to undergo the rapid growth that is required for transient bubbles

to form. Therefore, it is plausible that virtually all of the sonochemically active bubbles at 1057 kHz are HE-stable bubbles, which grow over many acoustic cycles via rectified diffusion. At the lower frequencies, transient and HE-stable bubbles can be expected to exist.

Finally, it is known that the rate of change of the surface area of the gas/solution interface will affect the rate of surfactant adsorption.[77] Therefore, it follows that the rate of change of the surface area of HE-stable bubbles will effect the ability of surfactants to establish equilibrium between the gas/solution interface of these bubbles and the bulk solution. Changes in both ultrasound intensity and frequency will affect the amplitude and rate of bubble oscillations, hence the rate of change of the surface area of the HE-stable bubble interface. To illustrate this effect, consider only the HE-stable bubbles that oscillate around an equilibrium radius (R_0) that is equal to the resonance radius (R_r). Choosing R_r as the equilibrium radius simply incorporates the effect of frequency on the magnitude of the HE-stable bubble radii (see Table 2) for the purposes of this exercise. The maximum and minimum oscillation radii of HE-stable bubbles around R_r are defined as R_{comp} for the compressed bubble and R_{exp} for the expanded bubble. Thus, we propose a simple calculation of the "time averaged rate of change of the surface area of the HE-stable bubbles during oscillations around R_r" [$\Delta A_s(R_{comp} \leftrightarrow R_{exp})_t$] calculated using eq 2:

$$\Delta A_s(R_{comp} \leftrightarrow R_{exp})_t = -8\pi R_r[(R_{comp})^2 - (R_{exp})^2] \quad (2)$$

Equation 2 was derived by dividing the change in surface area (ΔA_s) as the bubble expands from R_{comp} to R_{exp} by the time of the rarefaction cycle, $1/(2f_r)$, which is the approximate time of bubble expansion from R_{comp} to R_{exp}. At a given frequency, R_{comp} and R_{exp} are dependent on the ultrasound intensity ($P_{display}$). Some insight into the effect of $P_{display}$ on $\Delta A_s(R_{comp} \leftrightarrow R_{exp})_t$ at constant frequency can be obtained by arbitrarily choosing the oscillation amplitudes R_{comp} and R_{exp} to exist in the range of 10 to 50% of R_r (this arbitrary choice is discussed in more detail later). The calculated values of $\Delta A_s(R_{comp} \leftrightarrow R_{exp})_t$ for this range of oscillation amplitudes are shown in Table 2 for the frequencies considered in the current study. Given the above description of cavitation, there are a number of explanations for the results of this study that can be rejected, as described below.

(ii) Results of the Current Study in Relation to Cavitation—Rejected Hypotheses. A number of physical parameters can affect cavitation,[78] including the solution viscosity, vapor pressure, and gas solubility.[40] However, at such low concentrations of surfactants considered in this study, these physical parameters effectively remain constant. If the physical properties of the bulk solution had changed significantly with the addition of millimolar concentrations of surfactants to the solution, a plateau in the radical-scavenging yield would not have been observed (Figures 6 and 8).

When the frequency of sonolysis is increased from 47 to 1057 kHz, the number of bubbles in the solution increases.[73c] Furthermore, the magnitude of the resonance (R_r) and the maximum (R_{max}) bubble radii decrease, resulting in a decrease of the maximum collapse temperature (T_{max}),[73c] and it follows that a lower number of primary radicals are produced per bubble. It has also been proposed that a greater proportion of the primary radicals produced can reach the bubble interface because of the greater surface area−volume ratio of the smaller bubbles at higher frequencies.[45] Although the above changes affect the total number of primary radicals scavenged by the surfactants, these changes would not be expected to affect the relative number of primary radicals scavenged by SPSo compared to those scavenged by SDS.

Some experimental data seems to support the hypothesis that the presence of surfactants at the gas/solution interface changes cavitation bubble dynamics,[79,80] and a number of mechanisms have been proposed to explain these observations.[35,79−81] Collectively, these mechanisms involve changes to the following parameters in the presence of surfactant: the surface tension of the liquid, mass transfer between the bubble and the bulk solution, water condensation and evaporation, and microstreaming.[35,79−81] However, arguments against the importance of the effect of adsorption of *n*-alkyl chain surfactants on cavitation bubbles in relation to effects on sonoluminescence have been presented elsewhere.[37b] It was shown during the 358-kHz[37c] and 515-kHz[82] sonolysis of aqueous solutions exposed to air that the addition of millimolar concentrations of SDS (in the presence or absence of millimolar concentrations of NaCl) could not decrease the multibubble sonoluminescence spectral intensity below that of pure water. This was true even up to bulk solution concentrations of surfactant as high as 20 mM, which is over 2 times the critical micelle concentration of SDS! These observations are not direct evidence that bubble dynamics have not been altered by the presence of surfactants at the bubble interface. However, the results[37c,82] do present definitive evidence that the changes to bubble dynamics that may occur when millimolar concentrations of *n*-alkyl chain ionic surfactants are added to solution definitely do not hinder sonoluminescence, a very sensitive probe for the detection of changes in cavitation. The above discussion supports the hypothesis that the effects observed in the current study (Figures 9 and 10) cannot be explained in terms of the effect of SDS (or SPSo) on the dynamics of the cavitation bubbles. Instead, the current results must be explained in light of changes occurring to cavitation bubble dynamics due solely to changes in the intensity and frequency of ultrasound.

One possibility is that changes in the ratio of HE-stable to transient bubbles with varying frequency have created the effect in Figure 9. It has been shown that SDS (2 mM)[83] reaches equilibrium between the bulk and the gas/solution interface after more than 3 ms (approximately 700 μs was required for the interfacial concentrations of SDS to reach 50% of the equilibrium value).[84] Hence, from the bubble lifetimes shown in Table 2 for transient bubbles, surfactants would not reach equilibrium concentrations at the interface of transient bubbles. Most of the surfactant adsorbed to the interface of transient bubbles is probably that which was originally adsorbed at the gas/solution interface of the nucleation germ. Second, it is generally accepted that it becomes more difficult to create transient bubbles at higher frequencies.[40a,54,56,75] Thus, postulating that the adsorption of SPSo and SDS at the gas/solution interface was further from the concentrations expected at equilibrium at the lower frequencies because of a greater proportion of transient bubbles being present compared to high-frequency sonolysis appears plausible. However, this hypothesis can be discarded on the grounds that the ultrasound intensity has not affected the relative ability of SPSo to scavenge primary radicals compared to that of SDS (Figure 10). It would be expected that an increase in the ultrasound intensity from $P_{display} = 20$ to 60 W (Figure 7) would also have a considerable effect on the ratio of HE-stable to transient bubbles.[73f,75]

On the basis of the lifetimes of HE-stable bubbles compared to those of transient bubbles (Table 2), it can be concluded that the majority of surfactant accumulation occurred at the interface of HE-stable bubbles at all frequencies. This is also supported

by the observation that the ratio of HE-stable to transient cavities (by varying $P_{display}$, Figure 10) did not affect the radical-scavenging ability of SPSo relative to that of SDS. Thus, a plausible explanation for the results of the current study (Figure 9) is that the adsorption of SDS and SPSo at the gas/solution interface of cavitation bubbles is further from equilibrium as the frequency of sonolysis is decreased.

Note that from Figure 6b it is clear that the plateau concentrations of SDS were reached at $[SDS]_{bulk} = 2$ mM, whereas for SPSo the plateau was reached at $[SPSo]_{bulk} = 3$ mM. The critical micelle concentration (CMC) is the point at which micelles form in solution and maximum (i.e., saturation) surfactant concentrations are attained at the gas/solution interface. In the presence of 2 mM SDS in the bulk solution (CMC = 8.2 mM),[85] the gas/solution interface is ~70% saturated with surfactant at equilibrium.[86] This would be considerably higher than the amount of surfactant at the interface in the presence of just 3 mM SPSo (CMC = 990 mM)[85] in the bulk solution. Thus, it must be concluded that the surfactants are still far from equilibrium adsorption concentrations at the HE-stable bubble interface at 1057 kHz; however, adsorption appears to be facilitated at 1057 kHz in comparison to adsorption at the lower frequencies. The observation that a similar plateau was reached would indicate that SPSo and SDS reach similar limiting levels of adsorption at the gas/solution interface of cavitation bubbles, which is determined by the oscillations of HE-stable bubbles. This hypothesis is discussed in detail below.

(iii) Results of the Current Study in Relation to Cavitation—Accumulation of Surfactant at the Gas/Solution Interface of HE-Stable Bubbles. By arbitrarily choosing the ultrasound intensity-dependent limit of oscillations of HE-stable bubbles to lie within a minimum and maximum oscillation amplitude range of 10 to 50% of R_r, some insight can be gained with regard to the effect of frequency on $\Delta A_s(R_{comp} \leftrightarrow R_{exp})_t$ (Table 2). The sole reason for this arbitrary choice is to compare how $\Delta A_s(R_{comp} \leftrightarrow R_{exp})_t$ changes as a function of ultrasound frequency and intensity.

It can be seen in Table 2 that $\Delta A_s(R_{comp} \leftrightarrow R_{exp})_t$ *decreases* substantially as the frequency of sonolysis is *increased*. It follows that if the rate of change of the interfacial area of the HE-stable bubble decreases with increasing ultrasound frequency, then surfactant adsorption would be facilitated at higher ultrasound frequencies. This could explain why SPSo and SDS have reached similar limiting levels of adsorption at 1057 kHz but have not been able to accomplish this at the lower frequencies (Figure 9). However, from the arbitrary choice of HE-stable bubbles having oscillation amplitudes that lie within 10 to 50% of R_r at all frequencies, it can be seen in Table 2 that for a given frequency, significant changes in $\Delta A_s(R_{comp} \leftrightarrow R_{exp})_t$ also occur as the oscillation amplitude of the HE-stable bubble is varied from 10 to 50% (Table 2). Thus, this arbitrary range of oscillation amplitudes would not be consistent with the data showing that $P_{display}$ had no effect on the relative ability of the surfactants to adsorb at the gas/solution interface of cavitation bubbles at 354 and 1057 kHz (Figure 10).

This problem can be addressed by placing further constraints on the range of oscillation amplitudes that the HE-stable bubbles can acquire between $P_{display} = 20$ to 60 W at the different frequencies. For example, if HE-stable bubbles have $P_{display}$-dependent oscillation amplitudes of between 30 and 50% of R_r at 354 kHz, then the possible range in the values of $\Delta A_s(R_{comp} \leftrightarrow R_{exp})_t$ would now vary from 1.08×10^{-3} to 1.80×10^{-3} m^2 s^{-1} (see Table 2). However, because of the much shorter times available for expansion and contraction at higher frequencies, the oscillation amplitudes of HE-stable bubbles at 1057 kHz could be smaller. Hence, the $P_{display}$-dependent oscillation amplitudes may vary in a lower range, 10 to 20% of R_r, so that $\Delta A_s(R_{comp} \leftrightarrow R_{exp})_t$ would vary from between 0.12×10^{-3} to 0.24×10^{-3} m^2 s^{-1} (see Table 2). If this is the correct scenario, then it can be seen from the values of $\Delta A_s(R_{comp} \leftrightarrow R_{exp})_t$ above that the frequency would have a greater effect on $\Delta A_s(R_{comp} \leftrightarrow R_{exp})$ then the ultrasound intensity would at constant frequency.

In summary, when the frequency of sonolysis is increased, the rates of bubble oscillations also increase; however, the amplitude of oscillation decreases substantially. At 47 and 354 kHz, the amplitude of oscillation of HE-stable bubbles is so large that the rate of change of the interfacial area of the bubble is considerably greater in comparison to that at 1057 kHz. Therefore, the relative ability of SPSo to adsorb at the HE-stable bubble interface compared to that of SDS deviates from that expected at equilibrium to a greater degree at low frequencies compared to high frequencies. Increasing the ultrasound intensity at constant frequency also results in an increased rate of change of the interfacial area of HE-stable bubbles; however, this effect is much smaller compared to the effects of frequency changes. Thus, only changes in the frequency of ultrasound result in detectable variations of the relative ability of surfactants to accumulate at the gas/solution interface of HE-stable bubbles (Figure 9), whereas no effect is detected when the ultrasound intensity is varied (Figure 10).

Conclusions

In the current study, an ultrasound-independent frequency effect was observed. This observation was made possible by carefully choosing the "reference" and "test" sonochemical reactions to be so similar that only one variable was considered as a function of ultrasound frequency (i.e., the relative ability of SPSo and SDS to accumulate at the gas/solution interface of cavitation bubbles). It can be concluded that SPSo and SDS absorb more freely at HE-stable bubble interfaces mainly because of their longer lifetime compared to that of transient cavitation bubbles. At higher ultrasound frequencies, surfactant adsorption is facilitated at the gas/solution interface of HE-stable bubbles compared to that at lower frequencies. This could be due to *smaller* rates of change of the interfacial area of HE-stable bubbles at *higher* frequencies. However, the concentrations of SPSo and SDS at the gas/solution interface of HE-stable bubbles at all frequencies of sonolysis must still be far from the interfacial concentrations that would be expected under equilibrium conditions. To our knowledge, this study represents the first demonstration of a frequency effect that is independent of the ultrasound intensity. This suggests that for a given sonochemical setup this particular system may be considered for sonochemical studies involving frequency effects, without the need of establishing the elusive "constant ultrasound power" at different frequencies. The effect of the configuration of the sonolysis apparatus on the current results has not been established here. However, it would be of future interest to determine whether the frequency effect presented in this study is also independent of the configuration of the apparatus. If this were to be the case, then the ratio of the SPSo to SDS plateaus presented in Figure 9 would be standard for all sonochemical apparatus operating at the same ultrasound frequency.

Acknowledgment. We thank Dr. Sankaran Subramanian of the Radiation Biology Branch, NIH, for useful discussions. J.Z.S. gratefully acknowledges a Visiting Fellowship received

from the Fogarty International Center, NIH, under the exchange visitor program.

References and Notes

(1) Yim, B.; Nagata, Y.; Maeda, Y. *J. Phys. Chem. A* **2002**, *106*, 104−107.
(2) Theron, P.; Pichat, P.; Petrier, C.; Guillard, C. *Water Sci. Technol.* **2001**, *44*, 263−270.
(3) Yim, B.; Yoo, Y.; Nagata, Y.; Maeda, Y. *Chem. Lett.* **2001**, 938−939.
(4) Adewuyi, Y. G. *Ind. Eng. Chem. Res.* **2001**, *40*, 4681−4715.
(5) Destaillats, H.; Alderson, T. W.; Hoffmann, M. R. *Environ. Sci. Technol.* **2001**, *35*, 3019−3024.
(6) Vinodgopal, K.; Ashokkumar, M.; Grieser, F. *J. Phys. Chem. B* **2001**, *105*, 3338−3342.
(7) Weavers, L. K.; Malmstadt, N.; Hoffmann, M. R. *Environ. Sci. Technol.* **2000**, *34*, 1280−1285.
(8) Destaillats, H.; Hung, H. M.; Hoffmann, M. R. *Environ. Sci. Technol.* **2000**, *34*, 311−317.
(9) Suzuki, Y.; Warsito; Maezawa, A.; Uchida, S. *Chem. Eng. Technol.* **1999**, *22*, 507−510.
(10) Drijvers, D.; Van Langenhove, H.; Vervaet, K. *Ultrason. Sonochem.* **1998**, *5*, 13−19.
(11) Hoffmann, M. R.; Hua, I.; Hochemer, R. *Ultrason. Sonochem.* **1996**, *3*, S163−S172.
(12) Liao, Y. Q.; Wang, Q.; Xia, H. S.; Xu, X.; Baxter, S. M.; Slone, R. V.; Wu, S. G.; Swift, G.; Westmoreland, D. G. *J. Polym. Sci., Polym. Chem. Ed.* **2001**, *39*, 3356−3364.
(13) Xia, H. S.; Zhang, C. H.; Wang, Q. *J. Appl. Polym. Sci.* **2001**, *80*, 1130−1139.
(14) Ooi, S. K.; Biggs, S. *Ultrason. Sonochem.* **2000**, *7*, 125−133.
(15) Ding, T.; Wang, H.; Xu, S.; Zhu, J. J. *J. Cryst. Growth* **2002**, *235*, 517−522.
(16) Xie, Y.; Zheng, X. W.; Jiang, X. C.; Lu, J.; Zhu, L. Y. *Inorg. Chem.* **2002**, *41*, 387−392.
(17) Fujimoto, T.; Mizukoshi, Y.; Nagata, Y.; Maeda, Y.; Oshima, R. *Scr. Mater.* **2001**, *44*, 2183−2186.
(18) Mizukoshi, Y.; Takagi, E.; Okuno, H.; Oshima, R.; Maeda, Y.; Nagata, Y. *Ultrason. Sonochem.* **2001**, *8*, 1−6.
(19) Caruso, R. A.; Ashokkumar, M.; Grieser, F. *Colloid Surf., A* **2000**, *169*, 219−225.
(20) Mizukoshi, Y.; Fujimoto, T.; Nagata, Y.; Oshima, R.; Maeda, Y. *J. Phys. Chem. B* **2000**, *104*, 6028−6032.
(21) Okitsu, K.; Nagaoka, S.; Tanabe, S.; Matsumoto, H.; Mizukoshi, Y.; Nagata, Y. *Chem. Lett.* **1999**, 271−272.
(22) Mizukoshi, Y.; Oshima, R.; Maeda, Y.; Nagata, Y. *Langmuir* **1999**, *15*, 2733−2737.
(23) Barbour, K.; Ashokkumar, M.; Caruso, R. A.; Grieser, F. *J. Phys. Chem. B* **1999**, *103*, 9231−9236.
(24) Okitsu, K.; Mizukoshi, Y.; Bandow, H.; Yamamoto, T. A.; Nagata, Y.; Maeda, Y. *J. Phys. Chem. B* **1997**, *101*, 5470−5472.
(25) Mizukoshi, Y.; Okitsu, K.; Maeda, Y.; Yamamoto, T. A.; Oshima, R.; Nagata, Y. *J. Phys. Chem. B* **1997**, *101*, 7033−7037.
(26) Sostaric, J. Z.; Caruso-Hobson, R. A.; Mulvaney, P.; Grieser, F. *J. Chem. Soc., Faraday Trans.* **1997**, *93*, 1791−1795.
(27) Arakawa, K.; Hagisawa, K.; Kusano, H.; Yoneyama, S.; Kurita, A.; Arai, T.; Kikuchi, M.; Sakata, I.; Umemura, S.; Ohsuzu, F. *Circulation* **2002**, *105*, 149−151.
(28) Tachibana, K.; Tachibana, S. *Echocardiography-J. Cardiovasc. Ultrasound Allied Technol.* **2001**, *18*, 323−328.
(29) Sasaki, K.; Yumita, N.; Nishigaki, R.; Sakata, I.; Nakajima, S.; Umemura, S. *Jpn. J. Cancer Res.* **2001**, *92*, 989−995.
(30) Yumita, N.; Nishigaki, R.; Umemura, S. *J. Cancer Res. Clin. Oncol.* **2000**, *126*, 601−606.
(31) Mišík, V.; Riesz, P. *Ann. N.Y. Acad. Sci.* **2000**, *899*, 335−348.
(32) Mišík, V.; Riesz, P. *Free Radical Biol. Med.* **1999**, *26*, 936−943.
(33) Mišík, V.; Riesz, P. *Ultrason. Sonochem.* **1996**, *3*, S173−S186.
(34) Miyoshi, N.; Mišík, V.; Fukuda, M.; Riesz, P. *Radiat. Res.* **1995**, *143*, 194−202.
(35) Fyrillas, M. M.; Szeri, A. J. *J. Fluid Mech.* **1996**, *311*, 361−378.
(36) Sostaric, J. Z.; Riesz, P. *J. Am. Chem. Soc.* **2001**, *123*, 11010−11019.
(37) Sostaric, J. Z. Interfacial Effects on Aqueous Sonochemistry and Sonoluminescence. Ph.D. Thesis, The University of Melbourne, Melbourne, Australia, 1999: (a) Chapter 6, (b) pp 189−190, (c) p 180.
(38) Miyoshi, N.; Sostaric, J. Z.; Riesz, P., To be submitted for publication.
(39) *Ultrasound*: *Its Chemical, Physical and Biological Effects*; Suslick, K. S., Ed.; VCH: New York, 1988: pp 19−26.
(40) Mason, T. J.; Lorimer, J. P. *Sonochemistry*: *Theory, Applications and Uses of Ultrasound in Chemistry*; Ellis Horwood Limited: West Sussex, U.K., 1988: p 46.
(41) Sato, M.; Itoh, H.; Fujii, T. *Ultrasonics* **2000**, *38*, 312−315.
(42) Beckett, M. A.; Hua, I. *J. Phys. Chem. A* **2001**, *105*, 3796−3802.
(43) Lifka, J.; Hofmann, J.; Ondruschka, B. *Water Sci. Technol.* **2001**, *44*, 139−144.
(44) Ondruschka, B.; Lifka, J.; Hofmann, J. *Chem. Eng. Technol.* **2000**, *23*, 588−592.
(45) Hung, H. M.; Hoffmann, M. R. *J. Phys. Chem. A* **1999**, *103*, 2734−2739.
(46) Hua, I.; Hoffmann, M. R. *Environ. Sci. Technol.* **1997**, *31*, 2237−2243.
(47) Kang, J. W.; Hung, H. M.; Lin, A.; Hoffmann, M. R. *Environ. Sci. Technol.* **1999**, *33*, 3199−3205.
(48) Mark, G.; Tauber, A.; Rudiger, L. A.; Schuchmann, H. P.; Schulz, D.; Mues, A.; von Sonntag, C. *Ultrason. Sonochem.* **1998**, *5*, 41−52.
(49) Colussi, A. J.; Hung, H. M.; Hoffmann, M. R. *J. Phys. Chem. A* **1999**, *103*, 2696−2699.
(50) Dekerckheer, C.; Dahlem, O.; Reisse, J. *Ultrason. Sonochem.* **1997**, *4*, 205−209.
(51) Reisse, J.; Caulier, T.; Deckerkheer, C.; Fabre, O.; Vandercammen, J.; Delplancke, J. L.; Winand, R. *Ultrason. Sonochem.* **1996**, *3*, S147−S151.
(52) Petrier, C.; David, B.; Laguian, S. *Chemosphere* **1996**, *32*, 1709−1718.
(53) Didenko, Y. T.; Gordeychuk, T. V.; Koretz, V. L. *J. Sound Vibr.* **1991**, *147*, 409−416.
(54) Entezari, M. H.; Kruus, P. *Ultrason. Sonochem.* **1996**, *3*, 19−24.
(55) Gordeychuk, T. V.; Didenko, Y. T.; Pugach, S. P. *Acoust. Phys.* **1996**, *42*, 240−241.
(56) Entezari, M. H.; Kruus, P. *Ultrason. Sonochem.* **1994**, *1*, S75−S79.
(57) Didenko, Y. T.; Nastich, D. N.; Pugach, S. P.; Polovinka, Y. A.; Kvochka, V. I. *Ultrasonics* **1994**, *32*, 71−76.
(58) Petrier, C.; Jeunet, A.; Luche, J. L.; Reverdy, G. *J. Am. Chem. Soc.* **1992**, *114*, 3148−3150.
(59) Petrier, C.; Lamy, M. F.; Francony, A.; Benahcene, A.; David, B.; Renaudin, V.; Gondrexon, N. *J. Phys. Chem.* **1994**, *98*, 10514−10520.
(60) Frohly, J.; Labouret, S.; Bruneel, C.; Looten-Baquet, I.; Torguet, R. *J. Acoust. Soc. Am.* **2000**, *108*, 2012−2020.
(61) Faid, F.; Contamine, F.; Wilhelm, A. M.; Delmas, H. *Ultrason. Sonochem.* **1998**, *5*, 119−124.
(62) Suslick, K. S.; Hammerton, D. A.; Cline, R. E. *J. Am. Chem. Soc.* **1986**, *108*, 5641−5642.
(63) It should be noted that Reisse and co-workers recognized the difficulty in relating the sonochemical observations to how the ultrasound frequency affects the cavitation phenomenon.
(64) Sostaric, J. Z.; Mulvaney, P.; Grieser, F. *J. Chem. Soc., Faraday Trans.* **1995**, *91*, 2843−2846.
(65) Spinks, J. W. T.; Woods, R. J. *An Introduction to Radiation Chemistry*, 3rd ed.; Wiley-Interscience: New York, 1990.
(66) Atkins, P. W.; Symons, M. C. R. *The Structure of Inorganic Radicals; An Application of Electron Spin Resonance to the Study of Molecular Structure*; Elsevier: Amsterdam, 1967.
(67) Makino, K.; Mossoba, M. M.; Riesz, P. *J. Am. Chem. Soc.* **1982**, *104*, 3537−3539.
(68) Makino, K.; Mossoba, M. M.; Riesz, P. *J. Phys. Chem.* **1983**, *87*, 1369−1377.
(69) Alegria, A. E.; Lion, Y.; Kondo, T.; Riesz, P. *J. Phys. Chem.* **1989**, *93*, 4908−4913.
(70) Eastoe, J.; Dalton, J. S. *Adv. Colloid Interface Sci.* **2000**, *85*, 103−144.
(71) Ferri, J. K.; Stebe, K. J. *Adv. Colloid Interface Sci.* **2000**, *85*, 61−97.
(72) Henglein, A. Contributions to Various Aspects of Cavitation Chemistry. In *Advances in Sonochemistry*; Mason, T. J., Ed.; JAI Press Ltd.: London, 1993; Vol. 3; pp 17−83.
(73) Leighton, T. G. *The Acoustic Bubble*; Academic Press: London, 1994: (a) pp 312−316, (b) 407−408, (c) pp 489−492, (d) p 427, (e) p 183, (f) pp 332−335.
(74) Neppiras, E. A. *Phys. Rep.* **1980**, *61*, 159−251.
(75) Apfel, R. E. *J. Acoust. Soc. Am.* **1981**, *69*, 1624−1633.
(76) Suslick, K. S. *Sci. Am.* **1989**, *260*, 80−86.
(77) Warszynski, P.; Wantke, K. D.; Fruhner, H. *Colloid Surf., A* **2001**, *189*, 29−53.
(78) The parameters that are kept constant during the experiments are not discussed here.
(79) Stottlemyer, T. R.; Apfel, R. E. *J. Acoust. Soc. Am.* **1997**, *102*, 1418−1423.
(80) Crum, L. A. *J. Acoust. Soc. Am.* **1980**, *68*, 203−211.
(81) Yasui, K. *Phys. Rev. E: Stat. Phys., Plasmas, Fluids, Relat. Interdiscip. Top.* **1998**, *58*, 4560−4567.
(82) Ashokkumar, M.; Hall, R.; Mulvaney, P.; Grieser, F. *J. Phys. Chem. B* **1997**, *101*, 10845−10850.

(83) SDS (2 mM) is a plateau concentration in the current study (see Figures 6 and 8)
(84) Fainerman, V. B.; Makievski, A. V.; Miller, R. *Colloid Surf., A* **1994**, *87*, 61−75.
(85) Mukerjee, P.; Mysels, K. J. *Critical Micelle Concentrations of Aqueous Surfactant Systems*; U.S. Government Printing Office: Washington, DC, 1970; Vol. 36.
(86) Prosser, A. J.; Franses, E. I. *Colloid Surf., A***2001**, *178*, 1−40.